

# Analysis of Power Consumption in Multishaft Mixers

Xiao Wang, Maya Farhat, Louis Fradette,\* and Philippe A. Tanguy

URPEI, Department of Chemical Engineering, Ecole Polytechnique, P.O. Box 6079 Station CV, Montreal, Quebec H3C 3A7, Canada

**ABSTRACT:** New definitions of the Reynolds and power numbers proposed by Farhat, Fradette, and Tanguy (2008) for coaxial mixers were discussed and extended to some other types of multishaft mixers not considered previously. The results confirmed that these new correlations are also applicable for the dual shaft mixer configurations and the Superblend mixer. This universal applicability allowed the authors to experimentally investigate and compare the power consumption and the mixing time in the coaxial, the dual shaft, and the Superblend mixers based on uniform criteria. It was found that the Mixel TT–Anchor combination is the most power-efficient combination, whereas the Superblend mixer requires the most power. Besides, a general approach was introduced to predict the power constant of these multishaft mixers. Finally, the limitations of the new correlations were pointed out through the extension study of their applicability in Superblend and Rotor Stator–Paravisc dual shaft mixer.

## 1. INTRODUCTION

The quality of mixing in industrial reactors depends on various factors including, among others, the vessel volume, the physical properties of the ingredients, and the evolution of the rheology in the bulk. One flexible equipment proposed to cope with complex rheology is the multishaft mixer, which typically combines two or more impellers in a single vessel. This approach has seen rapid acceptance due to its flexibility dealing with widely varying viscosity conditions. A thorough literature review on coaxial mixers, a particular case of multishaft mixers, can be found in the work of Farhat et al.<sup>1</sup> On the basis of the compilation of previous studies, Farhat et al.<sup>1</sup> introduced new definitions for the Reynolds number and the power number in terms of impeller characteristic diameter and speed. These resulting power correlations were shown to be applicable for the coaxial mixer combining an anchor and either a radial impeller (Rushton turbine) or an axial impeller (Mixel TT). With respect to other types of multishaft mixers, several innovative studies have been carried out based on, for instance, dual shaft configurations<sup>2–5</sup> or Superblend mixers.<sup>6–8</sup> The design and the optimization of multishaft mixers are at present mainly based on empirical knowledge mostly because the specific investigations on such mixers are fairly new but also due to the controversy about what should be used as their characteristic parameters, owing to their inherent hydrodynamic complexity.

The present work aims at analyzing the power consumption of multishaft mixers and introducing a general approach to predict the power constant of multishaft mixers. This work is presented in three parts:

- 1) discussion and extension of the new correlations proposed by Farhat et al.<sup>1</sup> to some mixing configurations not considered in the first instance;
- 2) comparison and analysis of the power consumption, the mixing time and the mixing energy of three types of mixers operating in similar conditions;
- 3) assessment of the applicability of the newly proposed correlations.

## 2. MATERIALS AND METHODS

In this specific case, for the first mixer (Figure 1), the tank diameter was 0.38 m, the slow-speed peripheral agitator was an anchor of 0.36 m in diameter and the high-speed shaft could be fitted with either a Rushton turbine or a Mixel TT impeller of 0.2 m in diameter. Both shafts were connected to torque meters. This mixer was operated in both co- and counter-rotating modes of the impellers. Although the rotating direction does not have an impact on the hydrodynamics for the radial turbine Rushton turbine, it induces up or down pumping conditions for the axial turbine Mixel TT.

The second mixer was a 50 L dual shaft mixer as presented in the work of Barar Pour et al.<sup>2</sup> (Figure 2). It consisted of a tank of 0.4 m in diameter fitted with a slow-speed scraping Paravisc impeller of 0.34 m in diameter (Figure 2a). Here again, torque was measured on both shafts. Two configurations were studied by changing the high-speed off-centered impeller. The first impeller was a Deflo disperser of 0.08 m in diameter (Figure 2b) and the second Mixel TT of 0.09 m in diameter (Figure 1b). This mixer was operated only in the co-rotating mode, i.e., the impellers are moving in the same direction.

The third mixer was a 40 L Superblend mixer, as shown in Figure 3.

The tank was a 0.38 m polycarbonate cylinder fitted with a conical bottom. The overall liquid height was 0.44 m. The Superblend mixer is composed of a low-speed helical ribbon at the periphery (diameter of 0.36 m) and a high-speed Maxblend impeller in the center (diameter of 0.2 m). Two independent motors are used to drive the agitators so that both agitators can be rotated co- and counter-clockwise. In our setup, the power dissipated in the fluid could be measured by means of torque meters fitted on both shafts.

In all the experiments, the power input for each impeller was determined from the mechanical torque and the speed measurements as  $P = M2\pi N$ , where  $N$  is the shaft rotational

**Received:** August 5, 2013

**Revised:** December 20, 2013

**Accepted:** January 2, 2014

**Published:** January 2, 2014



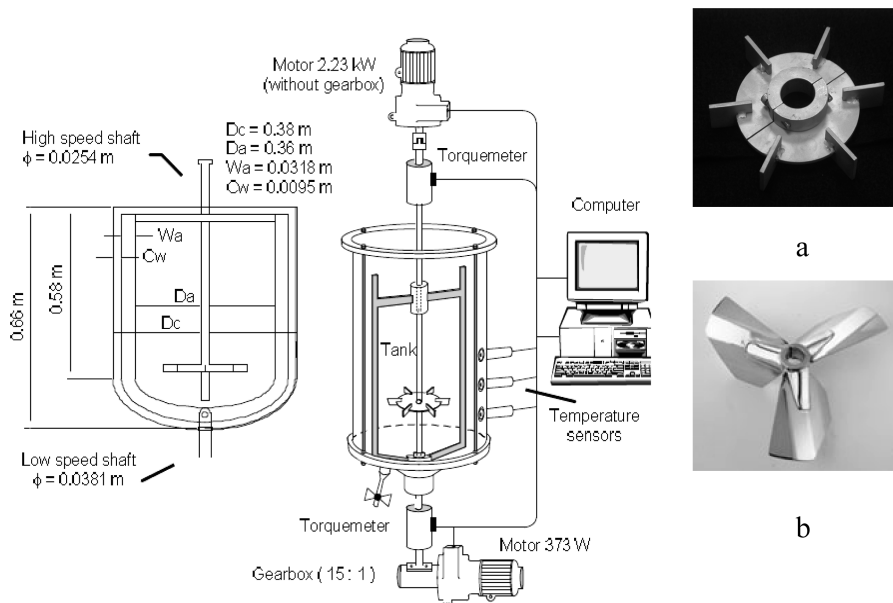


Figure 1. Coaxial mixer used in the work of Farhat et al.<sup>9</sup> (a) Rushton turbine; (b) Mixel TT.

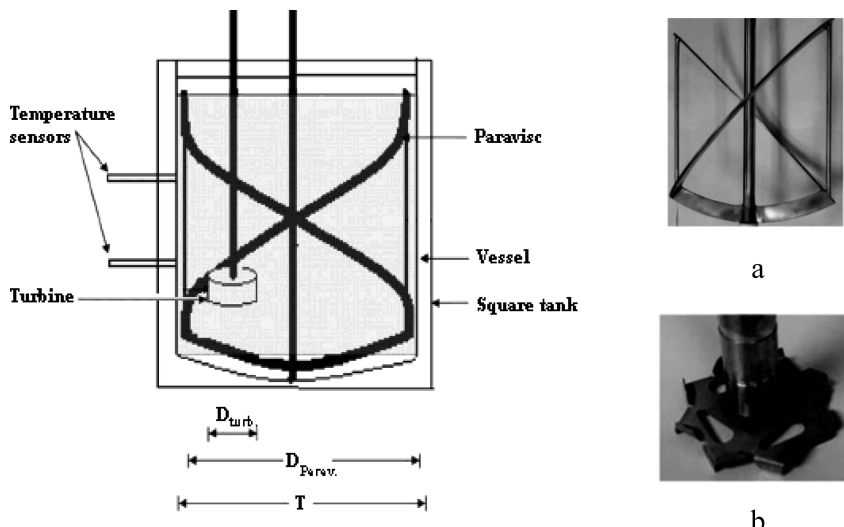


Figure 2. Dual shaft mixer used in the work of Barar Pour et al.<sup>2</sup> (a) Paravisc-type impeller; (b) Deflo disperser.

speed and  $M$  the corrected torque, i.e., after having subtracted the residual torque measured without fluid. Aqueous solutions of corn syrup were used as the working fluids. The rheological properties of the Newtonian fluids were determined using a Bohlin viscometer. The viscosities ranged from 0.1 to 200 Pa·s. The fluid viscosity measurements as well as the mixing experiments were performed at room temperature ( $\approx 22$  °C). The effect of temperature was accounted for by correcting the viscosity appropriately.

Mixing time was measured by means of a decolorization technique based on a fast acid–base reaction. An aqueous solution of 0.08% bromocresol purple was first poured into the fluid as an indicator. At a pH lower than 5.2, the fluid appears yellow and it turns purple at a pH higher than 6.8. As a typical procedure, 10 mL of 10 N NaOH was first put into the tank, which made the fluid purple. Then, 10 mL of 10 N HCl mixed with the working fluid to avoid viscosity variation was poured into the tank. This addition was made only after a homogeneous purple color was obtained in the tank. Starting

at the addition of HCl, the entire color-changing process was recorded by a video camera and, subsequently, an image processing technique developed by Cabaret et al.<sup>5,10</sup> was used to quantitatively determine the color evolution from which a macro mixing time can be obtained.

### 3. RESULTS

**3.1. Discussion on Power Correlation.** A number of studies have tried to characterize the power consumption of coaxial mixers by proposing different correlations with characteristic parameters.<sup>11,12</sup> In Farhat et al.,<sup>1</sup> new definitions of characteristic speed ( $N$ ), Reynolds number ( $Re$ ), and power number ( $N_p$ ) were introduced as shown below. Using the combination of an anchor and Rushton turbines with four different diameters, and an anchor and a single Mixel TT, they demonstrated that the power consumption obtained using these definitions could yield a single power curve regardless of the speed ratio, rotating mode and the high-speed impeller diameter.

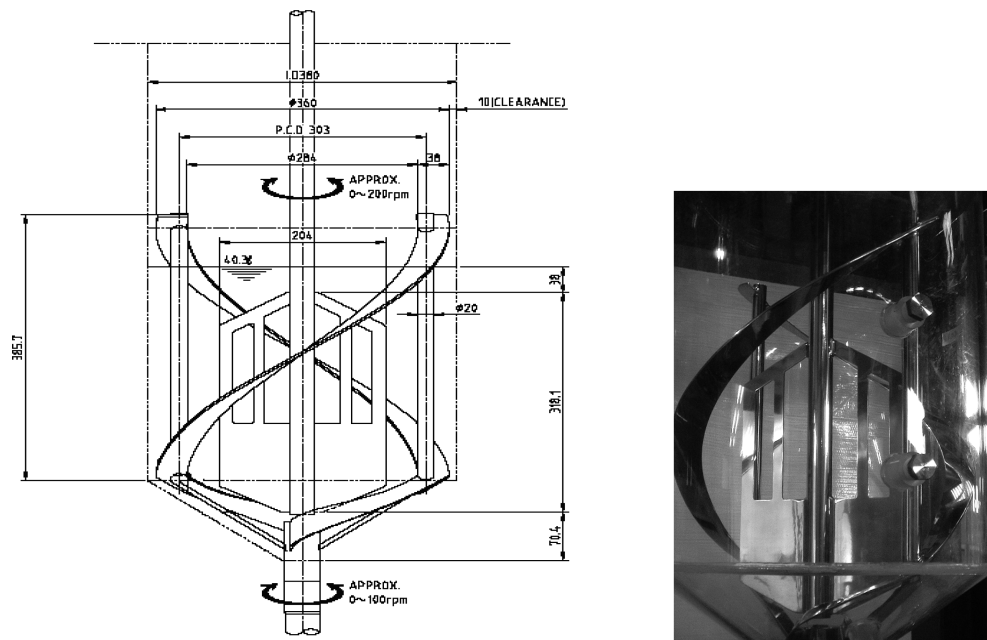


Figure 3. Superblend coaxial mixer experimental setup.

$$N = \frac{(N_i D_i + N_o D_o)}{D_i} \quad (1)$$

$$Re = \frac{\rho(N_i D_i + N_o D_o) D_i}{\mu} \quad (2)$$

$$N_p = \frac{P}{\rho(N_i D_i + N_o D_o)^3 D_i^2} \quad (3)$$

The above definitions are based on a weighing of the impeller tip speeds. Due to the fact that the high-speed impeller is dominant in the overall power consumption, using its diameter as the characteristic diameter is in agreement with the work of Foucault et al.<sup>12</sup> Because both agitators induce fluid flow, the contribution from each must be taken into account. In the co-rotating mode, they create circulation in the same direction, whereas in the counter-rotating mode, the discharge flows oppose each other. The maximum velocity generated by each agitator is always located at its tip and becomes almost zero close to the tank wall. Initially, it is expected that the velocity in the “antagonistic” region (in between the impellers) will be almost zero due to the counteraction of the impellers. Nevertheless, Figure 4 illustrates that these flow patterns show the addition of the speeds, not only in the co-rotating mode but also in the counter-rotating mode. Consequently, the total flow is almost equivalent in both rotating modes. This reality is reflected in the newly proposed correlations where the tip speeds are summed up for both rotating modes. Because the characteristic speed in both rotating modes is the same and the flow pattern is similar, it does not come as a surprise that the total power values are approximately the same at the same Reynolds number.

**3.2. Extensions of the Applicability of the Power Correlations.** To further assess the applicability of the newly proposed correlation, we verified its applicability to dual shaft mixers and the Superblend mixer. In Figure 5a, the power curves of the Deflo–Paravisc dual shaft mixer in co-rotating

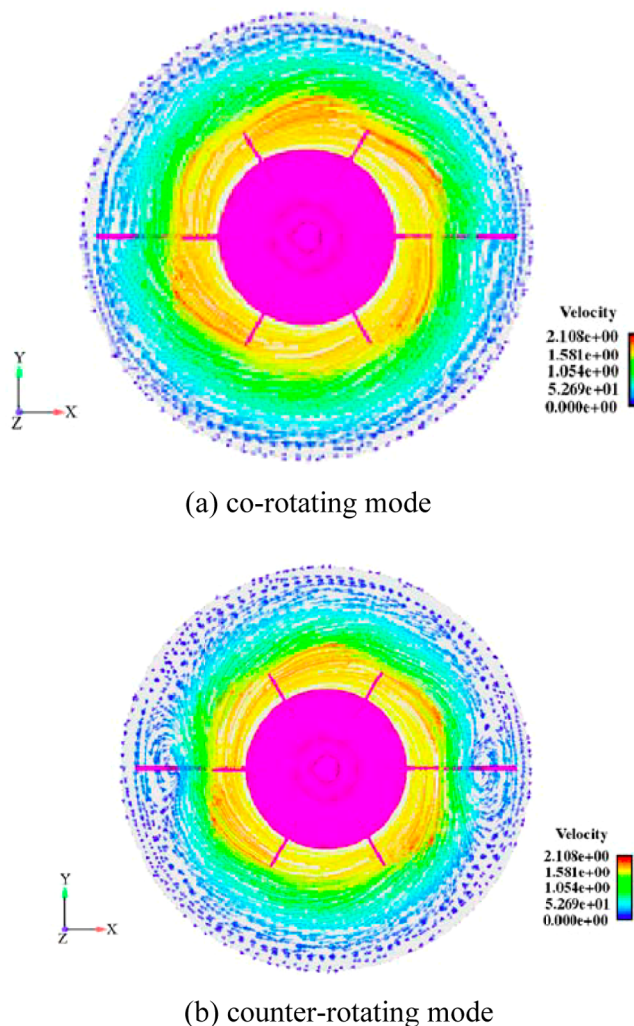
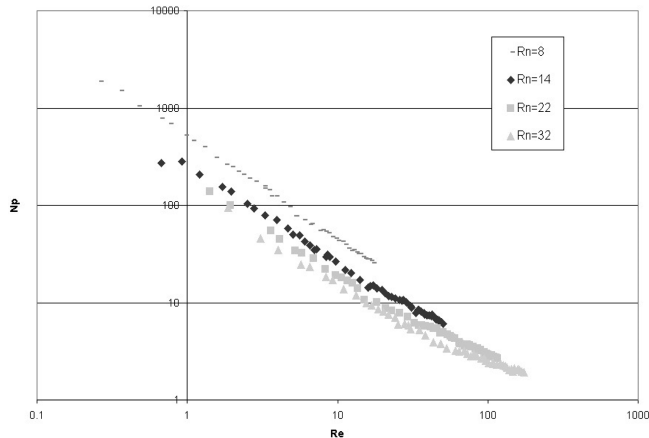
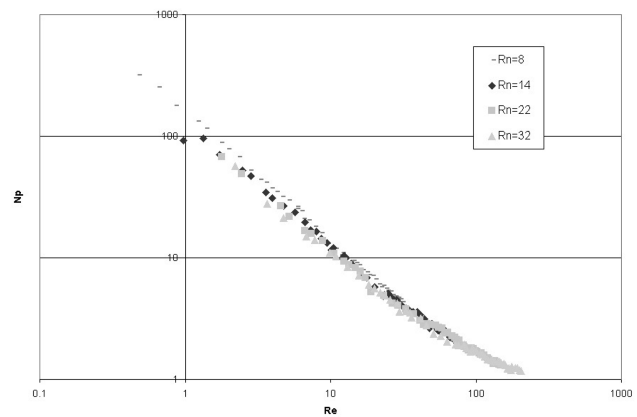


Figure 4. Flow patterns (tangential velocity, m/s) for the Rushton–Anchor configuration, plane XY is at Z = 0.2 m (Rivera et al.<sup>13</sup>).



(a) using the correlations from the work of Foucault et al. (2005)



(b) using the new correlations

**Figure 5.** Power curve for the Deflo-Paravisc dual shaft (a) using the correlations from the work of Foucault et al.;<sup>12</sup> (b) using the new correlations.

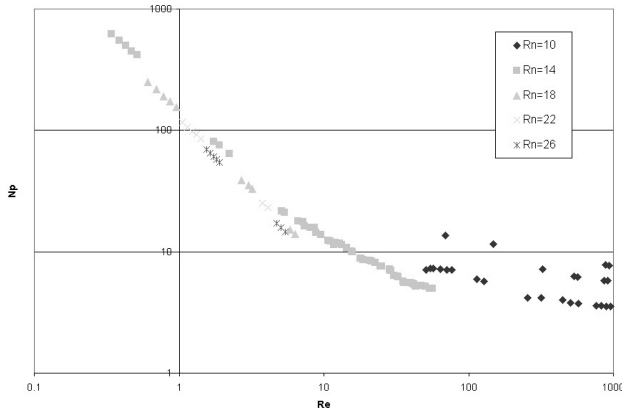
mode are shown using the definitions ( $N_{\text{co-rotating}} = N_i - N_o$ ,  $Re = \rho(N_i - N_o)D_t^2/\mu$ ) presented by Foucault et al.<sup>12</sup>

We can clearly see that the equations of Foucault et al. are not applicable to this dual shaft mixer, because the power consumption at each speed ratio still presents an independent curve. However, the power curves collapse onto a single curve that is independent of the various speed ratios when using eqs 2 and 3 as shown in Figure 5b. Very similar results were obtained for the Mixel TT-Paravisc dual shaft mixer in co-rotating mode as shown in Figure 6.

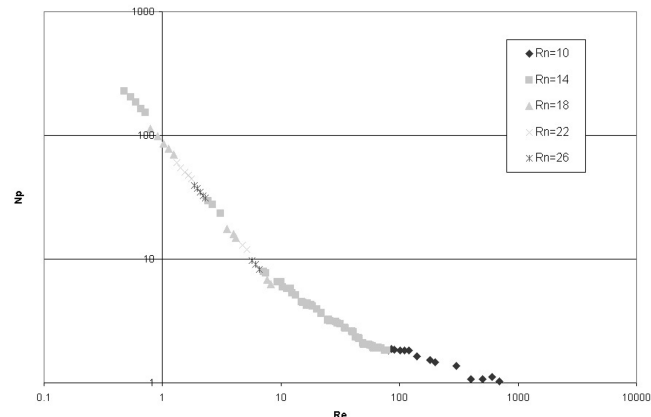
Taking advantage of the new correlations, a single power curve for the Superblend mixer regardless of speed ratio was obtained, as shown in Figure 7. In addition, the rotating mode did not have to be explicitly included in the power number calculations.

**3.3. Performance Comparison.** Obtaining single power curves for many different multishaft mixers makes it possible to compare the different mixers based on this “universal” Reynolds number. The following sections aim at comparing the various geometries of mixers and determine, on a unified basis, which geometry has the most to offer in terms of power constant and mixing time.

**3.3.1. Power Constant.** Derived from eqs 2 and 3, the definition of power constant in this work is shown as the following:



(a) using the correlations from the work of Foucault et al. (2005)



(b) using the new correlations

**Figure 6.** Power curve for the Mixel TT-Paravisc dual shaft (a) using the correlations from the work of Foucault et al.;<sup>12</sup> (b) using the new correlations.

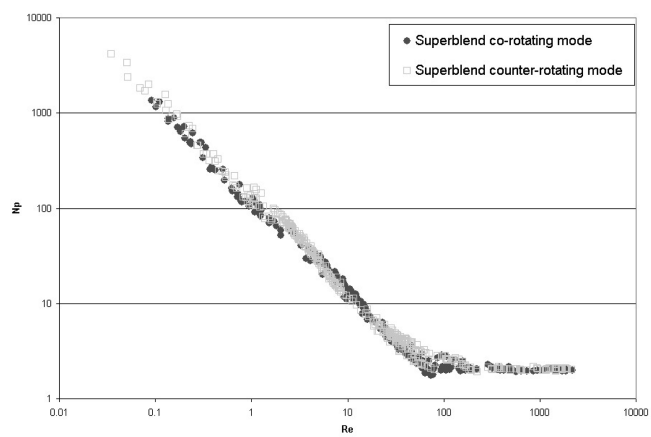


**Figure 7.** Power curve for the Superblend using the new correlations (Farhat et al.).<sup>7</sup>

$$K_p = Re \times N_p = \frac{P}{\rho(N_i D_i + N_o D_o)^2 D_i} \quad (4)$$

Table 1 shows the power constants for all the three mixers in co-rotating mode. It shows that the coaxial mixer consisting of the Mixel TT-Anchor combination has the lowest power constant (45), whereas the Superblend consumes the most power in the laminar regime (130). Meanwhile, as another

Table 1. Comparison of  $K_p$  for Multishaft Mixers

multishaft mixers	$K_p$ of high-speed impeller	$K_p$ of low-speed impeller	$K_p$ of multishaft mixer
coaxial Rushton–Anchor (L–L)	70	170	70
coaxial Mixel TT–Anchor (L–L)	45	170	45
dual shaft Deflo–Paravisc (L–H)	65	368	110
dual shaft Mixel TT–Paravisc (L–H)	45	368	60
Superblend (H–H)	200	370	130

proof of the power-efficient effect of Mixel TT, the power constant of Mixel TT–Paravisc (60) is remarkably lower than that of Deflo–Paravisc (110).

The fact that the Mixel TT–Anchor system was more efficient can be explained by the axial pumping effect of the Mixel TT (axial turbine). This pumping is far superior to the one generated by the Rushton turbine (radial turbine). On the other hand, the Mixel TT–Paravisc dual shaft mixer is less power-efficient than the Mixel TT–Anchor coaxial mixer. This can be explained by the existence of more effective impeller interactions or less counteraction between the Mixel TT and the anchor compared to that between the Mixel TT and the Deflo with the Paravisc. In all these regimes, the Superblend is the most power consuming mixer. Again, this does not come as a surprise because the Maxblend is bulkier than any of the turbines used.

We also compared the power constant of the high-speed impellers to the one of the multishaft systems when they are at high speed ratio ( $R_N > 10$ ) in Table 1 as well. The  $K_p$  values for the individual impellers composing the multishaft mixers are listed along with the  $K_p$  value of the multishaft mixer itself. Three cases can be seen: (1) both impellers have fairly low  $K_p$  (case Low–Low, i.e., L–L); (2) both impellers have high  $K_p$  (Superblend, case High–High, i.e., H–H); 3) the high-speed impeller with low  $K_p$  and the low-speed impeller with high  $K_p$  (dual shaft with RT/TT + Paravisc, case Low–High, i.e., L–H).

In the L–L case, the first observation is that the  $K_p$  of the Rushton or the Mixel TT alone equals that of the multishaft system. This behavior can be explained by the fact that the high-speed impeller plays the dominant role in the power consumption of the coaxial system, especially at high speed ratio. Indeed, the low-speed impeller mostly acts as a rotating baffle in that mode of operation. Moreover, in this work, the low-speed impeller is an anchor well-known for its lack of axial pumping. Therefore, its impact on the overall hydrodynamics is minimal and explains why the high-speed impeller alone is representative of the overall power consumption. On the basis of this result, we can easily predict the  $K_p$  of any coaxial mixer of that type (L–L), operating at high speed ratio, as the  $K_p$  value of the high-speed impeller. The simple calculation can be used when changing the type of high-speed turbine for example and where the geometry of the mixer remains the same.

In the case of Low–High, the overall power consumption is not as much dominated by the high-speed impellers only. In these configurations, the low-speed impeller is a Paravisc type and it contributes to the overall hydrodynamics, much more than an anchor can do. This results in a dual shaft power constant that is higher than that of the high-speed impeller and lower than that of the low-speed impeller (Paravisc–Deflo:  $65 < 110 < 368$ ; Paravisc–Mixel TT:  $45 < 60 < 368$ ). In these configurations, the  $K_p$  of the dual shaft system is close to the

one of the high speed impeller but always above. This can easily be interpreted as if the high-speed impeller is still dominant in the power consumption; the dominance is not as overwhelming as in the coaxial mixers. Hence, an intermediate  $K_p$  value is obtained. This intermediate value cannot be predicted from our results.

The case of the Superblend (H–H) is somehow puzzling at first glance. The  $K_p$  of the Superblend is lower than that of the individual impellers ( $200 > 130 < 370$ ). The Superblend is a coaxial mixer that possesses a high-speed impeller with high  $K_p$  combined to the contribution from the helical ribbon also with a high  $K_p$ . When the helical ribbon is static and the  $K_p$  of the Maxblend is obtained, the ribbon acts like a baffle that increases the  $K_p$  of the Maxblend. The opposite is also true when the  $K_p$  of the ribbon is obtained with the Maxblend being static in the tank: its  $K_p$  rose compared to a ribbon alone in a tank. When the helical ribbon is rotating along with the Maxblend, the interaction between the two tends to lower the overall power consumption. There is no doubt that the Maxblend is dominating the power consumption in this condition and the  $K_p$  of the Superblend should be close to 200, which is  $K_p$  of the Maxblend. Being different from other coaxial mixers, however, the gap between those two impellers is so small that the effect of power saving produced by helical ribbon leads the  $K_p$  of the Superblend to a much lower value. The behavior of the  $K_p$  value could also indicate an optimum operating speed ratio. This optimum has not been found, however.

**3.3.2. Mixing Time.** Figure 8 presents the dimensionless mixing time  $N \times t_m$  ( $t_m$ , mixing time) for all the three mixers in

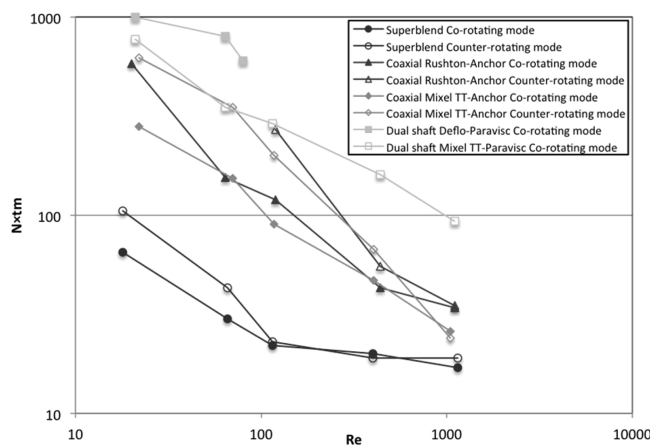


Figure 8. Dimensionless mixing time comparisons for all mixers.

different configurations and rotating modes as a function of the Reynolds number calculated from eq 2. It clearly shows that the Superblend mixer either in the co-rotating mode or in the counter-rotating mode requires much less time to reach complete mixing at the same  $Re$  value as other mixers. The coaxial mixer with both Rushton–Anchor and Mixel–Anchor configurations in co-rotating mode is always more efficient than that in counter-rotating mode. The dual shaft mixer performs the worst in terms of mixing time.

The uniform shear and efficiency of the Maxblend impeller has already been highlighted in a series of articles.<sup>14–18</sup> This combination of Maxblend impeller and double helical ribbon is proposed to be very efficient in deep laminar regime mixing because both impellers have good pumping capacities with highly viscous fluids. The coaxial mixer in both configurations

performs better than the dual shaft mixer. This result can be explained from the perspective of the diameter of the agitators. It is well-known that the mixing performance can be affected by the diameter ratio of the impeller to the tank in the laminar regime.<sup>19</sup> Herein, diameter ratio of the high-speed impeller to the tank in the coaxial mixer is about 0.5 and that of the dual shaft mixers just reaches 0.2. The introduction of a high-speed impeller into the dual shaft system is aiming at breaking the vortex, disperse and help to form a full circulation in the tank. Finally, as expected, the co-rotating mode is more efficient than the counter-rotating mode for all mixers, which is also supported by a number of previous studies.<sup>20–22</sup>

**3.3.3. Mixing Energy.** Aiming to assess the mixing efficiency of each mixer considering both the energy consumption and mixing time, the performances of these mixers are compared again in Figure 9 in terms of the dimensionless mixing energy,

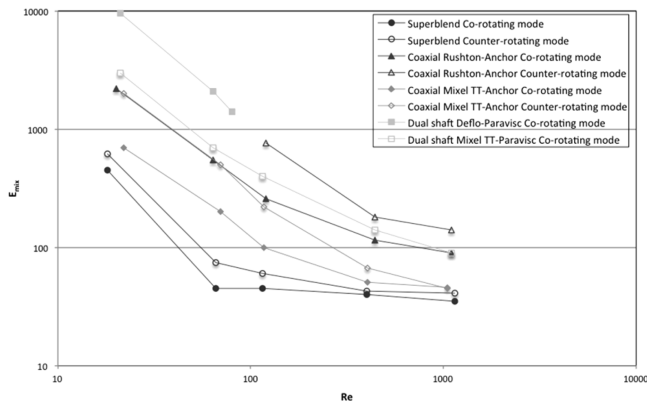


Figure 9. Dimensionless mixing energy comparisons for all mixers.

$E_{\text{mix}} = N_p \times N \times t_m$ , where we can clearly see the superiority of the Superblend mixer. Although this combination consumes more energy in comparison with other mixers, as shown in Table 1, its overwhelming performance on mixing time allows it to be the most efficient mixer in terms of mixing energy. In terms of mixing efficiency comparison, the coaxial mixers with Rushton–Anchor and Mixel–Anchor configurations follow the Superblend, and dual shaft Deflo–Paravisc mixer is still the worst. However, it is surprising that Mixel TT–Paravisc dual shaft becomes more efficient than the Rushton–Anchor coaxial mixer in counter-rotating mode when both power consumption and mixing time are taken into account.

On the other hand, Figure 9 not only allows comparison of the different mixers but it also allows comparison of the co- and counter-rotating modes. The performance of the co-rotating mode is, once again, superior to the counter-rotating mode for all tested configurations. As the power demands of different types of mixers are quite different, mixing energy allows us to compare their mixing performance taking both the effects of the power consumption and the mixing time into account.

**3.4. Limitations of the New Power Correlations.** We extended the assessment of the applicability of the new correlations to a dual shaft mixer provided with an off-centered rotor stator (VMI-Rayneri, France). The rotor stator is characterized by a strong dissipating capacity but a rather poor pumping contribution. Figure 10 shows the power curves for the Rotor Stator–Paravisc dual shaft mixer using the new correlations. In this figure, instead of a single curve, different power curves were obtained at different speed ratios, which

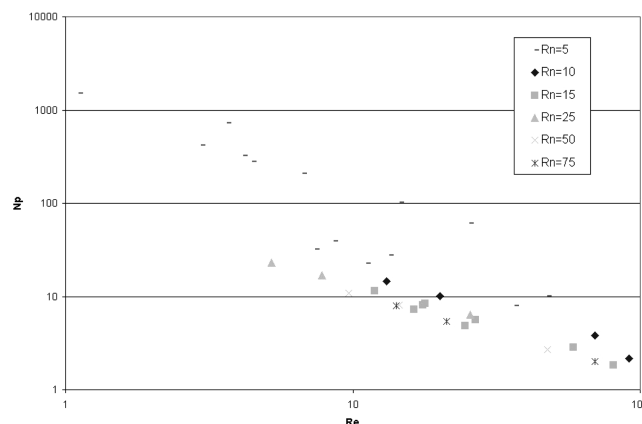


Figure 10. Power curve for the Rotor Stator–Paravisc dual shaft using the new correlations.

means the speed ratio still has influence on the power curve, which cannot be universalized by the new correlations.

This finding is consistent with the conclusion proposed by Wang et al.<sup>8</sup> They carried out the investigation of the effect of speed ratio on the power consumption of the Superblend mixer specifically at very low speed ratios ( $R_N = 1–8$ , whereas  $R_N > 8$  in the work of Farhat et al.<sup>7</sup>) and failed to attain a single curve for all speed ratios and modes as shown in Figure 11. Indeed, this figure presents the strong effect of speed ratio and rotating mode on the power consumption. It also shows that the helical ribbon is taking a non-negligible role in the power consumption at low speed ratio.

On the basis of the peculiar cases above, it can be concluded that the new correlations are applicable when the high-speed impeller is the largest contributor to the fluid circulation in the tank. The quantitative evaluation of this contribution can be done according to published work,<sup>23</sup> specifically using the proposed momentum number. The important aspect is that this hydrodynamically dominating impeller also dominates the power consumption. More specifically, the rotor stator discharge as a jet flow through stator teeth is the main dissipation mechanisms. This can hardly bring any axial pumping to the dual shaft system. The domination in the power consumption is determined not only by the configuration of each impeller but also by the speed ratio between them. The higher the speed ratio is, the higher the domination is. Because the previous results of coaxial mixers were also focused on high speed ratio, we can notice that, as for Rotor Stator–Paravisc dual shaft mixer or coaxial mixers at low speed ratio, the lack of pumping from high-speed impeller and the power contribution from the low-speed impeller causes the failure of the applicability of the new power correlations in such mixing systems.

#### 4. CONCLUSIONS

The first objective of this work was to discuss and extend the investigation of the applicability of the new correlations proposed by Farhat et al.<sup>1</sup> It was found that these correlations are well suited for dual shaft mixers and the Superblend. The second objective was to compare the power consumption, the mixing time, and the mixing energy of different mixers and introduce a general approach to predict the power constant of multishift mixers. The results showed that the Superblend mixer requires more power than all the other mixers, whereas the Mixel TT–Anchor combination is the most power-efficient.

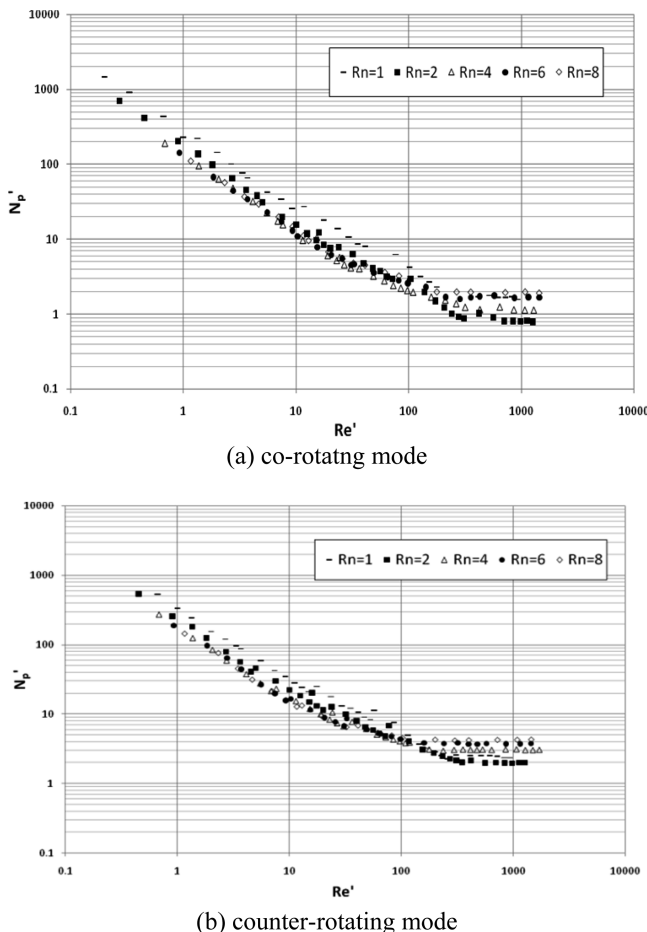


**Figure 11.** Power curves of Superblend mixer using the new correlations ( $N_p'$  and  $Re'$  are equivalent with  $N_p$  and  $Re$  presented in this work): (a) co-rotating mode; (b) counter-rotating mode (Wang et al.<sup>8</sup>).

On the other hand, the Superblend shows an excellent mixing efficiency in terms of mixing time and mixing energy outperforming both coaxial and dual shaft mixers. As another conclusion, the possibility of predicting the power constant of multishaft mixers was based on two assumptions: the speed ratio must be high enough to allow the high-speed impeller to dominate the power consumption and the interaction must be weak enough to avoid the interference from the low-speed impeller. Finally, the limitations of the new correlations were discussed through the extension application on Superblend at low speed ratios and Rotor Stator–Paravisc dual shaft mixer.

## AUTHOR INFORMATION

### Corresponding Author

\*L. Fradette. Tel.: 514-340-4711. Fax: 514-340-4105. E-mail: louis.fradette@polymtl.ca.

### Notes

The authors declare no competing financial interest.

## ACKNOWLEDGMENTS

The support of NSERC and the research consortium on Non-Newtonian Innovative Mixing Technologies is gratefully acknowledged.

## ABBREVIATIONS

- $D_a$  = diameter of the anchor (m)
- $D_c$  = diameter of the mixing tank (m)
- $D_i$  = diameter of the inner impeller (m)
- $D_o$  = diameter of the outer impeller (m)
- $K_p$  = power constant (–)
- $M$  = corrected torque (N·m)
- $N$  = rotational speed (1/s)
- $N_i$  = rotational speed of the inner impeller (1/s)
- $N_o$  = rotational speed of the outer impeller (1/s)
- $N_p$  = power number (–)
- $P$  = power (W)
- $Re$  = Reynolds number (–)
- $R_N$  = speed ratio between inner and outer impeller (–)
- $t_m$  = mixing time (s)
- $\mu$  = viscosity (Pa·s)
- $\rho$  = density (kg/m<sup>3</sup>)

## REFERENCES

- (1) Farhat, M.; Fradette, L.; Tanguy, P. A. Revisiting the performance of a coaxial mixer. *Ind. Eng. Chem. Res.* **2008**, *47* (10), 3562–3567.
- (2) Barar Pour, S.; Fradette, L.; Tanguy, P. A. Laminar and slurry blending characteristics of a dual shaft impeller system. *Chem. Eng. Res. Des.* **2007**, *85* (A9), 1305–1313.
- (3) Khopkar, A.; Fradette, L.; Tanguy, P. Hydrodynamics of a dual shaft mixer with Newtonian and non-Newtonian fluids. *Chem. Eng. Res. Des.* **2007**, *85*, 863–871.
- (4) Cabaret, F.; Rivera, C.; Fradette, L.; Heniche, M.; Tanguy, P. A. Hydrodynamics performance of a dual shaft mixer with viscous Newtonian liquids. *Chem. Eng. Res. Des.* **2007**, *85* (A5), 583–590.
- (5) Cabaret, F.; Bonnot, S.; Fradette, L.; Tanguy, P. A. Mixing time analysis using colorimetric methods and image processing. *Ind. Eng. Chem. Res.* **2007**, *46* (14), 5032–5042.
- (6) Kuratsu, M.; Nishimi, H.; Yatomi, R.; Sato, H.; Mishima, M. Mixing Reactor “Superblend” applied to wide range of viscosity. *Sumitomo Heavy Industries Technical Review* **1994**, *42* (124), 82–85.
- (7) Farhat, M.; Fradette, L.; Horiguchi, H.; Yatomi, R.; Tanguy, P. A. Experimental investigation of Superblend coaxial mixer. *Chem. Eng. J.* **2009**, *42* (11), 797–803.
- (8) Wang, X.; Fradette, L.; Takenaka, K.; Tanguy, P. A. Effect of operating parameters on the mixing performance of the Superblend coaxial mixer. *Ind. Eng. Chem. Res.* **2012**, *51* (4), 1826–1833.
- (9) Farhat, M.; Rivera, C.; Fradette, L.; Heniche, M.; Tanguy, P. A. Numerical and experimental study of dual-shaft coaxial mixer with viscous fluids. *Ind. Eng. Chem. Res.* **2007**, *46* (14), 5021–5031.
- (10) Bonnot, S.; Cabaret, F.; Fradette, L.; Tanguy, P. A. Characterization of mixing patterns in a coaxial mixer. *Chem. Eng. Res. Des.* **2007**, *85* (A8), 1129–1135.
- (11) Thibault, F.; Tanguy, P. A. Power-draw analysis of a coaxial Mixer with Newtonian and Non-Newtonian Fluids in the Laminar Regime. *Chem. Eng. Sci.* **2002**, *57*, 3861–3872.
- (12) Foucault, S.; Ascanio, G.; Tanguy, P. A. Power Characteristics in Coaxial Mixing: Newtonian and Non-Newtonian Fluids. *Ind. Eng. Chem. Res.* **2005**, *44*, 5036–5043.
- (13) Rivera, C.; Foucault, S.; Heniche, M.; Espinosa-Solares, T.; Tanguy, P. A. Mixing analysis in a coaxial mixer. *Chem. Eng. Sci.* **2006**, *61* (9), 2895–2907.
- (14) Yao, W.; Mishima, M.; Takahashi, K. Numerical Investigation on Dispersive Mixing Characteristics of Maxblend and Double Helical Ribbons. *Chem. Eng. J.* **2001**, *84*, 565–571.
- (15) Takahashi, K.; Horiguchi, H.; Mishima, M.; Yatomi, R. Mixing Characteristics in a Vessel Agitated by Large Paddle Impeller Maxblend. *Proceedings of the 12th European Conference on Mixing*, Bologna, Italy, 2006.
- (16) Takenaka, K.; Yatomi, R.; Morinaga, S.; Tanguy, P. A. Comparison of Solid–Liquid Mixing Performance between a Pitched

Blade Turbine and the Maxblend Impeller. *Proceedings of the 12th European Conference on Mixing*, Bologna, Italy, 2006.

(17) Yatomi, R.; Takenaka, K.; Morinaga, S.; Takahashi, K.; Tanguy, P. A. Large Paddle Impeller for Enhancing Surface Aeration: Application to Polymerization Reactor with Liquid Level Change. *Proceedings of the 12th European Conference on Mixing*, Bologna, Italy, 2006.

(18) Fradette, L.; Thomé, G.; Tanguy, P. A.; Takenaka, K. Power and Mixing Time Study Involving a Maxblend Impeller with Viscous Newtonian and Non-Newtonian Fluids. *Chem. Eng. Res. Des.* **2007**, *85*, 1514–1523.

(19) Paul, E. L.; Atiemo-Obeng, V. A.; Kresta, S. *Handbook of Industrial Mixing*; John Wiley & Sons, Inc.: Hoboken, NJ, 2004.

(20) Köhler, S.; Hemmerle, W. Analysis of the power characteristic of a coaxial agitator with varied diameter and speed ratio inner and outer mixing device. *11th European Conference on Mixing*, Bamberg, 2003.

(21) Foucault, S.; Ascanio, G.; Tanguy, P. A. Mixing times in coaxial mixers with Newtonian and non-Newtonian fluids. *Ind. Eng. Chem. Res.* **2006**, *45* (1), 352–359.

(22) Foucault, S.; Ascanio, G.; Tanguy, P. A. Coaxial Mixer Hydrodynamics with Newtonian and non-Newtonian Fluids. *Chem. Eng. Technol.* **2004**, *27* (3), 324–329.

(23) Machado, M. B.; Nunhez, J. R.; Nobes, D.; Kresta, S. M. Impeller Characterization and Selection: Balancing Efficient Hydrodynamics with Process Mixing Requirements. *AIChE J.* **2012**, *58* (8), 2573–2588.